

Faraday Discussions

Accepted Manuscript



This manuscript will be presented and discussed at a forthcoming Faraday Discussion meeting. All delegates can contribute to the discussion which will be included in the final volume.

Register now to attend! Full details of all upcoming meetings: <http://rsc.li/fd-upcoming-meetings>



This is an *Accepted Manuscript*, which has been through the Royal Society of Chemistry peer review process and has been accepted for publication.

Accepted Manuscripts are published online shortly after acceptance, before technical editing, formatting and proof reading. Using this free service, authors can make their results available to the community, in citable form, before we publish the edited article. We will replace this *Accepted Manuscript* with the edited and formatted *Advance Article* as soon as it is available.

You can find more information about *Accepted Manuscripts* in the [Information for Authors](#).

Please note that technical editing may introduce minor changes to the text and/or graphics, which may alter content. The journal's standard [Terms & Conditions](#) and the [Ethical guidelines](#) still apply. In no event shall the Royal Society of Chemistry be held responsible for any errors or omissions in this *Accepted Manuscript* or any consequences arising from the use of any information it contains.

Solar energy utilization in the direct photocarboxylation of 2,3-dihydrofuran using CO₂.

Michele Aresta^{1,2} Angela Dibenedetto^{2,3}, Tomasz Baran^{2,4}, Szymon Wojtyła⁴, Wojciech Macyk⁴

¹ ChBE, 4 Engineering Drive 4, NUS, Singapore 117585, SG; ² IC²R, Tecnopolis, via Casamassima km3, Valenzano 70018, Bari, IT; ³ CIRCC, Via Celso Ulpiani 27, Bari 70126, IT; ⁴ Faculty of Chemistry, Jagiellonian University in Kraków, Ingardena 3, 30-060 Kraków, PL

Introduction

Today, the introduction of a carboxylic group into an organic molecule occurs *via* synthetic methodologies characterized by low Carbon Fraction Utilization-CFU and high Carbon Footprint-CF. We have done a critical analysis of such issue long time ago and suggested that the direct carboxylation of C-H bonds (Eq. 1) represents one of the most effective ways to reduce the CO₂ emission and save fossil carbon.^{1,2} Such new syntheses may require a quite different approach than thermal reactions. In fact, a critical barrier that can occur for reaction, represented by C-H activation, must be overcome. The use of the photochemical technology may be of a great help supposed that photocatalysts able to activate the C-H bond using visible light are developed (Eq. 1).



On the other hand, CO₂ can be used as a source of carbon for the production of C₁ and C_n energy rich molecules, a process that also would be of a great interest supposed that fossil carbon is not used for providing the necessary energy for the reduction to occur and hydrogen is sourced from water or waste organics. Also in this case, the use of solar energy as primary energy source would be of fundamental importance.³

We have started a programme on the photochemical conversion of CO₂ using newly synthesized semiconductor-based photocatalysts that are able to operate under visible and/or solar light and have applied such systems to a number of reactions implying CO₂ conversion: either fixation into organic substrates of the entire molecule or reduction to C₁ and C_n molecules using water or abundant and cheap polyols as a source of hydrogen.

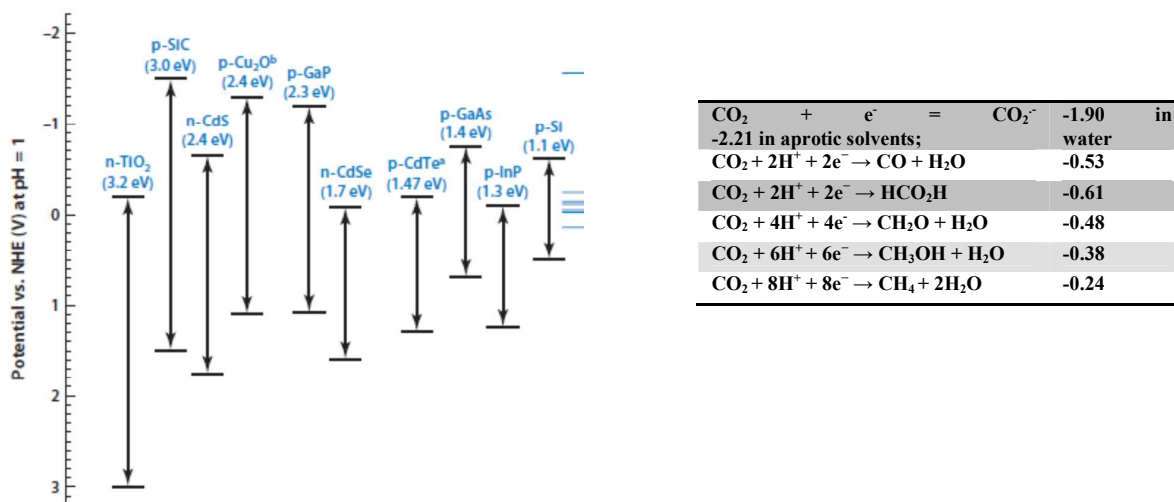


Figure 1: Comparison of the band gap energies of some semiconductors with the reduction potentials of CO₂ in aqueous solutions (pH = 1) for selected one- and multi-electron transfer processes.⁴

Figure 1 shows the matching of some semiconductors band gap and CO₂ reduction potentials in $2ne^-$ transfer processes in water compared to the higher energy $1e^-$ transfer.⁴

In this paper we recall the concept on which the catalysts are based on and present some very recent applications in both carboxylation reactions and CO₂ reduction. We discuss new results relevant to the carboxylation of a quite intriguing substrate, 2,3-dihydrofuran (2,3-DHF).

The new-concept photocatalysts and their application

The photocatalysts have been engineered by carrying out a surface modification of semiconductors such as TiO₂, ZnS and several others. As Fig. 1 shows, TiO₂ has a band gap energy of 3.2 eV that makes it not particularly suited for visible light utilization in CO₂ conversion. In fact, TiO₂ alone is better used under UV irradiation in oxidation processes that convert recalcitrant pollutant organics either in water or in air, thus producing CO₂. Moreover, due to a high oxidation potential of holes photoinduced in the valence band of titanium dioxide, reoxidation of the reduction product is plausible. The use of UV-light in CO₂ conversion would also not represent an efficient use of solar light, making the process both economically not viable and environmentally not acceptable. Nevertheless, it is possible to modify the spectral properties of titanium dioxide in several modes, as shown in Figure 2.

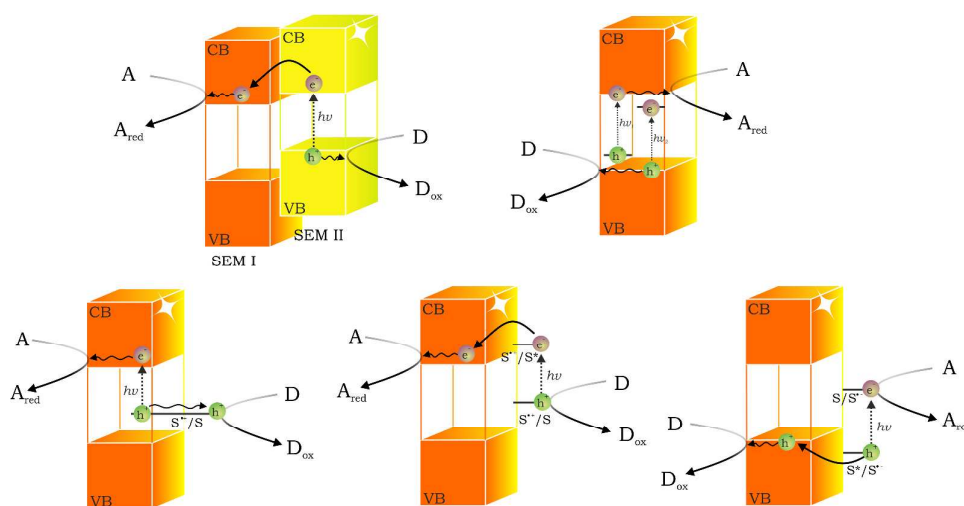


Figure 2: Mechanisms of wide band gap semiconductors photosensitization. A - formation of composite semiconductors, B - bulk doping resulting in formation of acceptor or donor levels, C - direct photosensitization (optical charge transfer), D - dye-photosensitization involving an electron injection to the conduction band from the excited photosensitizer, E - dye-photosensitization involving a hole injection to the valence band from the excited photosensitizer.

Modifications of semiconductors with species that are either “hole” (to the VB) or “electron” (to the CB) injectors may sensibly extend the spectral response of the photocatalysts and enhance their use with exploitation of solar light. Such concept may be applied to a number of semiconductors which do not absorb in the visible region, but more in the UV. So, TiO₂ modified with fluorochromates has been advantageously used in the reduction of NAD⁺ into NADH used as an “ e^- and H^+ ” vector to enzymes which reduce CO₂ to methanol.⁵⁻⁷

Another approach to enhance solar light utilization is to increase the quantum efficiency of processes driven by near-UV light (e.g. within the range of 320-400 nm) instead of questing for broadening the spectral response of the wide band gap semiconductors. This goal can be achieved

for instance by a surface functionalization of semiconductors with co-catalysts improving efficiency of charge separation and interfacial electron transfer processes. For example, nano-particles of elemental platinum deposited on the surface of TiO₂ act as electron sinks and enhance photoreduction of the adsorbed electron acceptor (e.g. O₂).⁸⁻¹¹ A similar methodology was successfully applied by us to zinc sulfide photocatalysts. As mentioned above, ZnS is an interesting photomaterial having the band gap energy larger than TiO₂ (3.6 vs 3.2 eV). Due to its redox properties, it may have a good potential for C-H activation. Unfortunately, ZnS alone does not show a good photoactivity. However, we have synthesized ZnS decorated with Ru nanoparticles¹² and used it for the carboxylation of C-H bonds having a different activation energy: either activated CH₂ moieties as in CH₃COCH₂COCH₃ (acac) or terminal CH₃, as shown in eq. 2.



In this photochemical process the formation of the radical anion CO₂⁻ has been demonstrated to be the key issue. The photomaterial used (ZnS) has the correct band gap energy for its generation, while Ru enhances the light harvesting capacity and drives the carboxylation reaction under sunlight irradiation. It is worth to note that acetylacetone can be carboxylated using chemical catalysts (typically a base such as the phenate anion) and affords only CH₃COCH(COOH)COCH₃. The use of the photocatalyst enables the activation of the C-H bond of the terminal methyl group, affording the terminal carboxylic acid CH₃COCH₂COCH₂COOH. Noteworthy, the C-H bonding energy is quite different in the CH₂ and CH₃ moieties. The former is activated due to tautomerism that brings the hydrogen onto the oxygen atom (Eq. 3). In the presence of bases the OH moiety is deprotonized and prompted to interact with CO₂. The terminal-CH₃ moiety is not activated and does not react in thermal reactions, but it does in photochemical processes.



ZnS decorated with ruthenium and *p*-type photocatalysts built on the same concept have been found to be active in the photoreduction of carbon dioxide to formic acid and carbon monoxide¹³ in protic solvents. *p*-Type semiconductors, in contrast to *n*-type materials, have rarely been studied for carbon dioxide conversion. We have found that wide-bandgap semiconductors (like CuI and NiO) characterized by a bandgap energy of 3.6-4.0 eV and a very low potential of the conduction band edge (in the range of -3.0 to -3.4 V vs. SHE) or also materials having a bandgap energy equal to 3.1 eV and the potential of conduction band edge of -2.1 V vs. SHE can be usefully applied in the photoreduction of CO₂.¹⁴ For example, under full solar light irradiation using isopropanol as hole scavenger CO₂ was reduced to CO, CH₄ and/or HCOOH. The preparation method (annealing temperature) plays a key role in determining the activity of the catalyst and its selectivity towards one of the products.

Results and discussion

Characterization of the catalysts

The properties of the Ru@ZnS-A and Ru@ZnS-B used in this work were already published^{12,13}. Here we report some new additional properties recently determined, namely the diffuse reflectance spectra and the photocurrent measurement, useful for determining the spectral region within which the catalysts are active, and the EDX analysis. Band gap energies were estimated from diffuse reflectance spectroscopy. Obtained spectra (reflectance, *R*, vs. wavelength, *λ*) have been transformed to Kubelka-Munk function (KM) according to the equation: KM = (1 - *R*)²/2*R* (Fig. 3). Spectra of bare ZnS and materials decorated with ruthenium are similar, i.e. ruthenium does not influence the absorption onset. The energy of band gap was calculated

according to Tauc theory as published elsewhere.^{12,13} ZnS-A shows a smaller bandgap energy (3.47 eV) than ZnS-B (3.64 eV). Materials decorated with ruthenium (0.5% of Ru) have the band gap energies of 3.57 and 3.65 eV for Ru@ZnS-A and Ru@ZnS-B, respectively. Prepared materials offer strong reduction properties (for example, the conduction band edge of ZnS-B is *ca.* -2.5 V *vs.* SHE) as learnt from spectroelectrochemical measurements published elsewhere.¹³

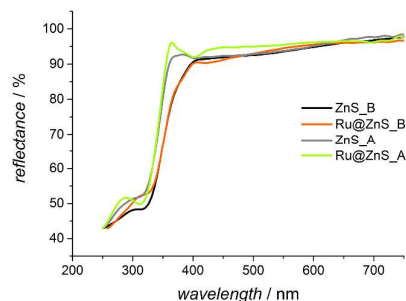


Figure 3: Diffuse reflectance spectra of the synthesized photocatalysts transferred to Kubelka-Munk function.

UV-Vis analysis nicely corresponds to the results of photocurrent measurements. Irradiation of ZnS-A-covered electrode with near-UV-VIS light (solar light) results in an anodic photocurrent generation (375 nm track), as shown in Fig. 4. The use of only visible light decreases the intensity of photocurrent (see wavelength 405 and 465 nm in Fig. 4). Application of light of longer wavelengths, 520, 595 and 630 nm, did not result in photocurrent generation.

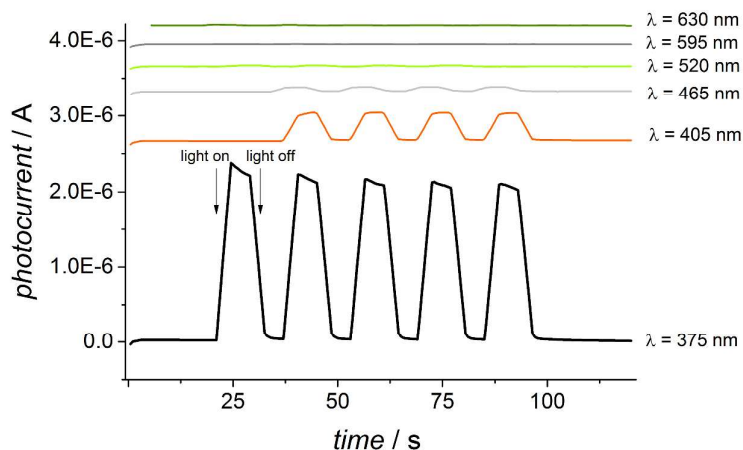


Figure 4: Photocurrent measurements: ZnS-A electrode irradiated with chopped light of 375, 405, 465, 520, 595, 630 nm wavelength.

The characterization of materials has been done by EDX analysis. Energy-dispersive X-ray spectra of ZnS-A and 1%Ru@ZnS-A are shown in Fig. 5. Both materials show typical signal of zinc and sulphur. Moreover, spectrum of 1%Ru@ZnS-A shows also signals assigned to ruthenium (2.69 and 19.27 keV). Raman spectroscopy excluded the formation of ruthenium(IV) oxide, since bands at 515 and 626 cm^{-1} , characteristic for this compound (RuO stretching modes) were not found, and this is in accordance with the XRD features of the materials,¹² previously published, which confirm the presence of Ru(0).

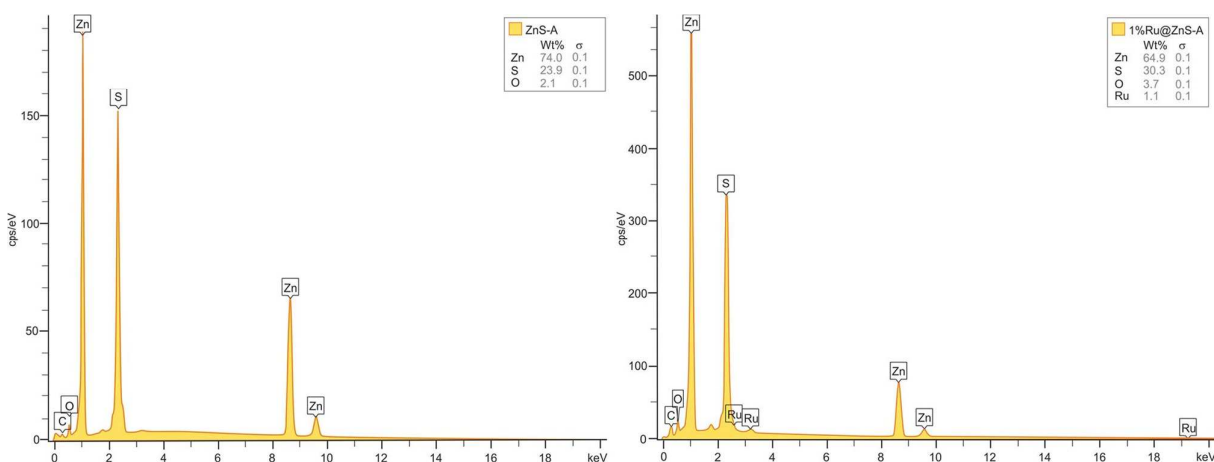


Figure 5. Energy-dispersive X-ray spectra of ZnS-A and 1%Ru@ZnS-A

The SEM image of Ru@ZnS-A (Fig. 6) shows that the material is composed of irregular aggregates of various sizes in the range from several nanometers up to 4 micrometers. DLS measurements prove that the average particle sizes are in the range of hundreds nanometers. SEM-EDX analysis proves the chemical composition of the material. All materials have relatively high specific surface areas (BET measurements) in the range of 55-105 m²g⁻¹, as published elsewhere.¹² The specific surface area of ZnS samples decorated with ruthenium is reduced when compared to bare materials.

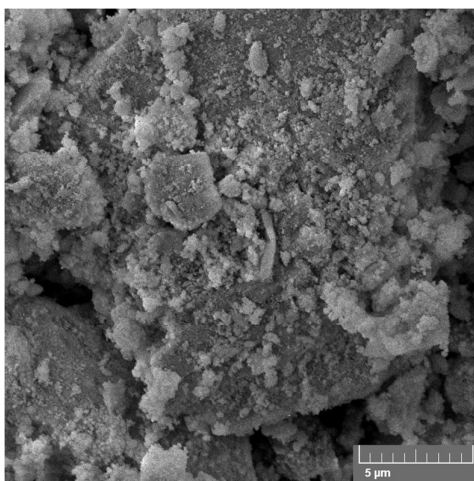


Figure 6: SEM of Ru@ZnS-A.

The target molecule and the observed reactions

In this paper we focus on the discussion of the photoconversion of an intriguing molecule, such as 2,3-dihydrofuran (2,3-DHF) (Fig. 7), at room temperature under inert gas or in the presence of CO₂ dissolved in aprotic or protic solvents.

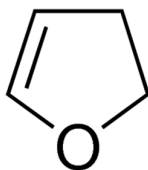


Figure 7: The 2,3-dihydrofuran molecule.

DHF is an interesting molecule as it contains a multiplicity of bonds having quite different energies. Table 1 shows the nature of bonds and their average energies.

Table 1: Bonds in 2,3-dihydrofuran and average energy in kJ/mol.

Bond	Number of bonds	Average energy kJ/mol	Ref.
sp^3C-sp^3C	1	346	¹⁵
sp^3C-sp^2C	1	386-390	¹⁶
sp^2C-sp^2C	1	610	¹⁵
sp^3C-H	4	411	¹⁷
sp^2C-H	2	422	¹⁸
sp^3C-O	1	358	¹⁵
sp^2C-O	1	418	¹⁹

The molecule has, thus, several reactive sites. Despite such complexity, it is foreseeable that the most reactive position will be the allylic $-CH_2-$ moiety, corresponding to the lower energy of the C-H bond, while C-C and C-O bond splitting may occur as secondary events (Table 1). However, in principle, H-extraction should occur, and occurs, at C-4, affording an allylic radical (Fig. 8). In order to check whether the photocatalyst would be able to promote the C-H bond cleavage, we have carried out a cyclic-voltammetry (CV) analysis. The CV measurements on a solution of 2,3-DHF are shown in Fig. 9. The voltammogram shows an irreversible peak at 1.35 V versus the non-aqueous silver electrode (Ag/Ag^+), corresponding to the oxidation of 2,3-DHF. The oxidation potential of 2,3-DHF (1.55 V vs. SHE) is lower than the potential of the ZnS valence band edge (1.8 V vs SHE²⁰), thus the photoinduced oxidation of 2,3-DHF by VB holes is thermodynamically possible.

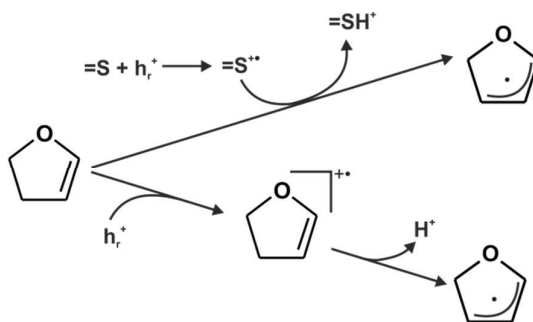


Figure 8: Radical formation in 2,3-DHF upon irradiation

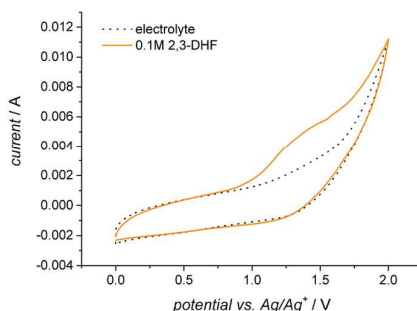


Figure 9: Cyclic voltammogram of 0.1 mol L⁻¹ 2,3-dihydrofuran in acetonitrile with lithium perchlorate (0.1 mol L⁻¹) as the electrolyte. Scan rate: 50 mV s⁻¹.

Such species can evolve in two different ways, (Fig. 10) affording either 2,5-dihydrofuran (2,5-DHF) or, *via* a C-O splitting and structural rearrangement, the formyl-cyclopropane molecule (F-Cyp) or even the linear crotonaldehyde (C-ald). Such photoinduced-isomerization products have been observed when 2,3-DHF was directly irradiated using UV-light.¹⁸

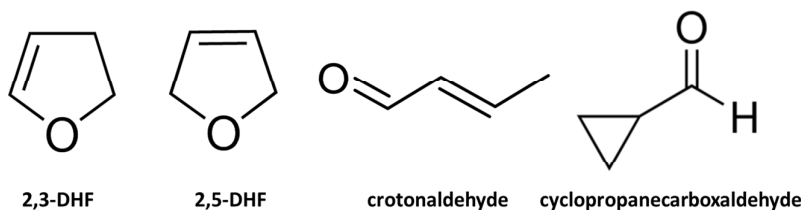


Figure 10: 2,3-DHF and products of its photocatalytic isomerization (inert atmosphere).

We show now that white (solar) light in presence of a photocatalyst can induce the isomerization. This adds a complexity to the system as one can ask if the interaction of the substrate with CO₂ will occur prior or after isomerization of the substrate and, thus, whether carboxylated forms of the rearrangement products can also be expected. Therefore, we have investigated the reactivity of the pure substrate and of it in the presence of CO₂ under the same experimental conditions (solvent, radiations, irradiation time, temperature, concentration). The study was carried out at a double scale: at a micro-scale in a pressurized NMR tube and in a larger photoreactor having a volume of 10 mL allowing sample withdrawal for GC analysis. Moreover, in order to establish if proton donors may influence the reaction, two different solvents were used, chloroform and methanol. We shall discuss the behaviour of 2,3-DHF in the two solvents separately, comparing the role of Ru@ZnS-A and Ru@ZnS-B.

Photocarboxylation in chloroform

Figure 11a shows the modification of the ¹³C NMR spectrum of 2,3-DHF under irradiation in a Ar atmosphere in chloroform in presence of Ru@ZnS-A and Fig. 11b shows the same system when Ru@ZnS-B is used. Noteworthy, within 2 h of irradiation in the presence of Ru@ZnS-A all starting substrate is converted (disappearance of resonances at 146, 99.5, 69.5 and 29.3 ppm typical of 2,3-DHF). Two major products are formed, namely: 2,5-DHF (signals at 104 and 63 ppm) and formylcyclopropane, identified through the signals at 205, 31 and 14 ppm. Crotonaldehyde, the alternative isomerization product derived from ring-opening, is absent as its resonances at 194.4, 154.3, 134.6 and 18 ppm are not found in the spectrum.²¹ Other very minor products are also formed (*ca.* 1% yield), while signals of ethanol are present since the beginning, most probably an impurity derived from the work-up of the photocatalysts. Interestingly, the use of Ru@ZnS-B increases the amount of formylcyclopropane, while producing the same isomerization products. It is

worth to note, that the NMR spectra do not show any change with respect to starting 2,3-DHF in absence of irradiation and in presence of the photocatalyst.

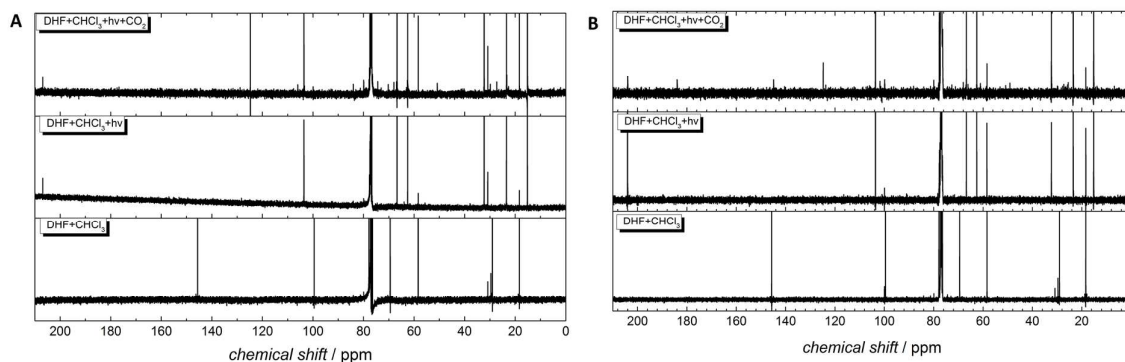


Figure 11: ^{13}C -NMR spectra of 2,3-DHF and after 2 h using Ru@ZnS-A (11A) and Ru@ZnS-B (11B) as photocatalysts: the starting product is quantitatively converted into isomerization products. In absence of CO_2 , carboxylated products are not formed.

Figure 11 presents the products formed in CHCl_3 when the photoconversion is carried out under 0.7 MPa of CO_2 in a high pressure NMR-sapphire tube using Ru@ZnS-B as photocatalyst. (Ru@ZnS-A) gives the same products, but at a lower concentration. Besides the signals due to the isomerization products, it is quite evident the insurgence of some new signals, some of which can be ascribed to species formed upon incorporation of CO_2 . In particular, the signals at 178, 144, 100, 62 and 50 ppm are due to the new species. A careful comparison of the ^{13}C -spectra of the reaction solution with those of the photoisomerization products found under Ar and then of the expected carboxylation products, brings to the conclusion that the major photocarboxylation product is 2,5-dihydrofuran-2-carboxylic acid (2-COOH-2,5-DHF). Such species has ^{13}C -NMR signals at 184 (COOH), 104 (C=C), 63 (CH₂) and 60 (CH-COOH) ppm. The absence of the signal at 140 ppm (characteristic of the O-bonded C in the O-CH=CH- moiety) confirms the isomerization of the starting material. A simulation of the ^{13}C -NMR spectrum made using CS Chem Draw Ultra 6 (Cambridge Software Corporation) shows that 2-COOH-2,5-DHF (Fig. 14a) has signals at 176, 129, 89 and 68 ppm, while 4-COOH-2,3-DHF (Fig. 14b) has computed signals at 177, 144, 100, 80 and 32 ppm. Finally, 2-COOH-1-formyl-cyclopropane has computed peaks at 204, 184, 36 and 6-15 ppm. The signals found in the ^{13}C -spectrum of the mixture irradiated with visible light in the presence of Ru@ZnS-B shows, in addition to the signals of 2,5-DHF and 1-formyl-cyclopropane, two series of new signals at: 184, 126, 81 and 68 ppm due to 2-COOH-2,5-DHF and lower signals attributable to 2-COOH-2,3-DHF at 184, 145, 102, 80 and 29 ppm. The absence of signals in the high part of the spectrum excludes the formation of the carboxylated form of 1-formyl-cyclopropane. The formation of the two carboxylated isomers can be explained with the coupling of the radical shown in Fig. 6 with the $\text{CO}_2^{\cdot-}$ radical anion. The new C-C bond is formed at C-2, and the double bond migrates to the 3-4 carbons or to the 4-5 carbons, the latter with a less favourable energetics as it implies H-migration. As reported above, 2-COOH-2,3-DHF is present in a lower concentration. Besides the signals of the products reported above, weak resonances due to THF and furan are also found, as occurs also in solutions irradiated in absence of CO_2 . A new signal due to methanol also appears (50 ppm) not found in absence of CO_2 , and this is quite interesting but not surprising as we have shown that CO_2 can be reduced to methane, formic acid or methanol under irradiation in the presence of the ZnS photocatalysts or others (such as CuI).¹³

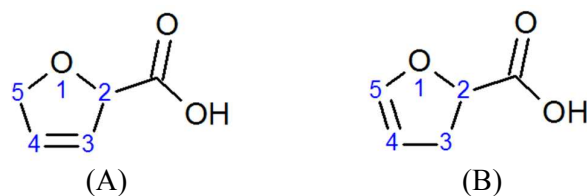


Figure 12: A) 2-COOH-2,5-DHF and B) 2-COOH-2,3-DHF

In order to get further information on the compounds formed, we have taken the $^1\text{H-NMR}$ spectrum of the mixture. This results to be a quite complex spectrum due to the many signals of the various isomers. The only significant signals are those of the aldehydic (9.75 ppm in CDCl_3) and carboxylic groups (11.3 ppm in CDCl_3 , not seen in CD_3OD most probably because of hydrogen bonding and H-D exchange that causes broadening).

In order to confirm the structural features of the carboxylated forms obtained through the multinuclear NMR, a GC-MS analysis of the reaction solution in methanol produced on a large scale was carried out that has allowed the identification of the various products. Several peaks were found in the GC of the solution irradiated in absence and presence of CO_2 , corresponding to the isomers described above. Under CO_2 the peak of the 2-COOH-2,3-DHF appeared, attributed on the basis of its fragmentation showing m/z values at: 114 (molecular peak), 85, 69, 45 (carboxylic group) and 41.

Carboxylation in methanol

The carboxylation in methanol has features different from those of the same reaction in CHCl_3 . A single carboxylated isomer is formed in this solvent, namely 2-COOH-2,3-DHF. This product is also formed in higher concentration than in chloroform, reaching over 25% of the total of the starting product, after 10 h with 1%Ru@ZnS-A as photocatalyst (Fig. 13B compares the various photocatalysts: ZnS-A, 1%Ru@ZnS-A, ZnS-B and 1%Ru@ZnS-B). The accumulation of carboxylated products over 10 h can be explained assuming that:

1. The isomerisation is fast and the isomerized product can be then carboxylated. This is not the case as discussed in next sub-chapter.
2. The isomerisation rate in methanol is slower than in chloroform or the lifetime of the radical shown in Fig 8 is longer in methanol so that a more extended carboxylation is observed with time, with higher selectivity.

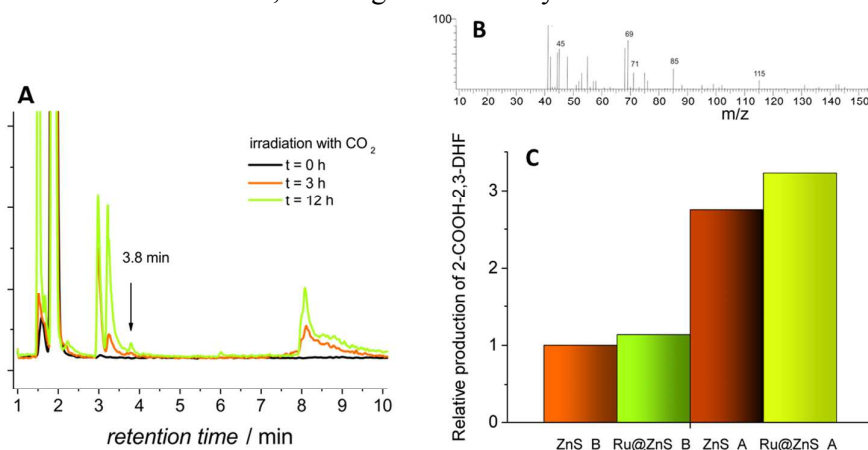


Figure 13: GC-MS analysis of the reaction solution during photocatalytic carboxylation of 2,3-DHF in methanol. A) Gas-chromatograms of samples withdrawn at different times during the photocatalytic tests in methanol using 1%Ru@ZnS-A as a photocatalyst with irradiation time 0, 3 and 12h, B) the MS spectrum on the peak at 3.8 min and C) the relative formation of 2-COOH-2,3-

DHF in the presence of ZnS-A (set equal to 1), 1%Ru@ZnS-A, ZnS-B and 1%Ru@ZnS-B after 10 hours of irradiation of a 2,3-DHF solution in methanol.

In order to collect data on the formation rate of the carboxylated product and on the activity of the catalysts, we have carried out extended irradiations of the solution up to 12 h and compared the catalysts. Figure 13 reports an example of the evolution of the chromatograms with time, the MS spectrum of the peak at 3.8 min due to 2-COOH-2,3-DHF and the relative activity of the different photocatalysts. Figure 13C clearly shows that the Ru-decorated ZnS materials are more active than bare sulphides. Using Ru@ZnS-A as photocatalyst and collecting data at fixed intervals of time (30 min) over 12 h it was possible to get preliminary information about the kinetics of conversion of the starting material. Figure 14 shows the percentage of conversion of 2,3-DHF into 2-COOH-2,3-DHF with time. It is interesting to note that at the time of 12 h all the starting materials was converted either into the isomerisation product or its carboxylated form, as demonstrated by ^{13}C NMR.

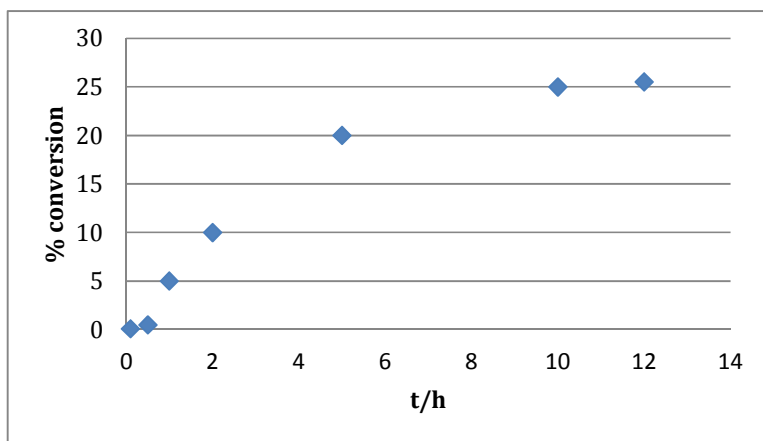


Figure 14: Photoconversion of 2,3-DHF into 2-COOH-2,3-DHF using Ru@ZnS-A as photocatalyst

Does the carboxylation occur concurrently with the photoisomerisation or after it?

As reported above, the only carboxylation product observed in CHCl_3 are 2-COOH-2,3(or 2,5)-DHF while no carboxylated forms of F-Cyp were found. The question came to our mind whether the carboxylation is concurrent with the isomerisation or follows such step. We have carried out a simple experiment to answer such question. We have first irradiated the 2,3-DHF solution under argon in CHCl_3 in presence of the photocatalyst Ru@ZnS-B or Ru@ZnS-A and, when the photoconversion of 2,3-DHF into 2,5-DHF and 1-formyl-cyclopropane was complete, CO_2 was admitted and the irradiation continued. The analysis of the reaction mixture after irradiation (2 h) showed that there was no further conversion of 2,5-DHF nor 1-formyl-cyclopropane inferring, thus, that the carboxylation occurs on the radical species shown in Fig. 8 more than on the products of photoisomerization. The carboxylation of the substrates formed upon isomerisation of 2,3-DHF takes place under quite different conditions than those described in this paper.

Conclusions

The irradiation of a solution of 2,3-DHF in CHCl_3 in the presence of Ru@ZnS-B under inert atmosphere causes isomerization of the starting product into 2,5-DHF and 1-formyl-cyclopropane. This reaction proceeds through the formation of allylic radicals (hydrogen abstraction from 2,3-DHF), identical to that formed in the reaction of 2,5-DHF oxidation by valence band holes generated upon irradiation of ZnS and CdS.^{22–25} Since the radical is stabilized by its two resonance structures, its lifetime is sufficient to enable bimolecular reactions. When methanol is used, the photoisomerization reaction requires a longer time.

When the irradiation is carried out under CO₂ atmosphere in CHCl₃, the carboxylation of the substrate occurs affording two isomeric products, namely 2-COOH-2,3-DHF and 2-COOH-2,5-DHF. The carboxylation occurs by coupling CO₂^{•-} radical anion with the allylic radical. The formation of CO₂^{•-} radical under the operative conditions has been confirmed by our recent studies involving spin-trapping and EPR measurements.²⁶ The generation of this very reactive radical is thermodynamically feasible due to high reduction abilities of electrons excited to the conduction band of zinc sulphide. Moreover, the presence of ruthenium nanoparticles enhances adsorption of carbon dioxide and improves the charge separation, what reflects in diminished recombination efficiency and the pronounced CO₂^{•-} formation.²⁶ When the photocarboxylation is carried out in methanol, 2-COOH-2,3-DHF is formed as the only product. This has allowed to carry out preliminary kinetic studies and calculate the photocarboxylation yield to be 25% after 10 h.

The photocarboxylation process discussed here is another example of a possible application of photocatalytic systems in the synthesis of chemicals. Although the overall efficiency of the process can be improved, the actual photoconversion is quite interesting (25 % of 2,3-DHF converted after 10 h, or 0.025 M) and mimics a reductive path of photosynthesis (reduction of carbon dioxide) utilizing the UV part of the solar radiation.

Experimental part

Synthesis of photocatalyst

Zinc sulphide (ZnS-A) was prepared according to methods published elsewhere.¹² Under argon atmosphere, using Schlenk's system, a solution of Na₂S (0.1 mol) in 25 mL of distilled water was added dropwise to the aqueous solution of ZnSO₄ (0.1 mol, 25 mL). The mixture was stirred for twenty four hours, filtrated, washed with water to neutrality and dried at room temperature under vacuum. Another sample of zinc sulphide (ZnS-B) was also prepared under nitrogen atmosphere. A solution of sodium hydroxide (10 g) in distilled water (20 mL) was added dropwise to a solution of ZnSO₄ (0.01 mol, 20 mL), as already described.¹² The primarily formed solid Zn(OH)₂ was dissolved as [Zn(OH)₄]²⁻. Afterwards, 40 mL of a thiourea solution (1.52 g) was added. The mixture was heated to 353 K for 48 h. After separation via centrifugation the powder was washed with H₂O and dried at 333 K. Ruthenium nanoparticles were deposited as follows. 1 g of ZnS was suspended in an aqueous solution of RuCl₃·xH₂O (10 mL, 10 mM) under argon atmosphere. A concentrated ethanol solution of NaBH₄ was added dropwise (in a big excess) under ultrasonic agitation. Then the powder was filtered off and washed with water under argon, dried and stored under nitrogen atmosphere.

Characterization of materials

Diffuse reflectance spectra of photocatalysts were measured using a UV-vis spectrophotometer (UV-3600 type, Shimadzu), equipped with an integrating sphere (15 cm diameter). 25 mg of analysed samples were ground with 0.5 g of BaSO₄. Barium sulphate was also used as the reference material. Hydrodynamic particle diameters were measured using Zetasizer NanoZS (Malvern). Scanning electron microscope (Vega 3 LMU, Tescan) was equipped with LaB₆ cathode. EDX spectra were recorded using the EDX detector (Oxford Instruments, X-act, SDD 10 mm²). The photoelectron spectra were measured using monochromatized aluminium AlK_α source (E = 1486.6 eV) and a low energy electron flood gun (FS40A-PS) to compensate the charge on the surface of non-conductive samples. A typical three-electrode set-up was employed for photocurrent analysis. The electrolyte solution was 0.1 M KNO₃. Platinum and Ag/AgCl were used as auxiliary and reference electrodes, respectively. The working electrodes were prepared by casting the samples onto ITO conductive foil. Light emitting diodes of various wavelengths (*Instytut Fotonowy*) were used as light sources. The measurements were collected using the potentiostat (PGSTAT 302N, Autolab).

Cyclic voltammetry

CV experiments were carried out using BioLogic SP-150 potentiostat. The measurements were collected at the scan rate of 100 mV/s. The electrochemical cell consisted of three electrodes: the glassy-carbon electrode (working electrode), the nonaqueous Ag/Ag⁺ (reference electrode) and platinum wire (counter electrode). The reference electrode was prepared by placing a clean silver wire into an electrolyte (0.01 M tetrabutylammonium perchlorate in acetonitrile) containing silver ions (0.01 M AgNO₃). The electrodes were placed in a Teflon cuvette filled with 0.1 mol dm⁻³ LiClO₄ solution in anhydrous acetonitrile. Oxygen was thoroughly removed from the electrolyte by purging with argon before (15 min) and during the experiment.

Photocatalytic tests

2,3-dihydrofuran was a Sigma-Aldrich product and was carefully distilled under reduced pressure prior to photocatalytic tests. It was stored at 4°C and used for up to 30 days after distillation. Chloroform was dried with alumina, distilled and stored under nitrogen atmosphere. Methanol was distilled under nitrogen atmosphere, dried with molecular sieves and distilled again. The photocatalyst (1 g dm⁻³) was suspended (by sonication) in the solvent (5 or 10 mL) and the organic substrate (0.1 mol dm⁻³ unless otherwise stated) was added. CO₂ was bubbled through the suspension for 3 minutes to remove oxygen and afterwards the mixture was closed under an elevated pressure of carbon dioxide (7-8 bar) in sapphire tube reactor, unless otherwise stated. Photocatalytic tests were carried out in a closed reactor using a XBO-150 lamp as the light source equipped with a cut-off filter (360 nm). Samples of the reaction mixture were collected periodically, filtered through syringe filters and analysed. The progress of the reaction was monitored by GC-MS (Shimadzu QP5050) equipped with DB 5 MS 30 m capillary column. Nuclear Magnetic Resonance-NMR experiments were carried out with a 400 MHz Varian INOVA apparatus and 600 MHz Bruker Advance.

Acknowledgements

IC²R srl is acknowledged for having made available the photocatalytic equipment. Authors thank Anna Regiel-Futyra for SEM measurements. The support from the Foundation for Polish Science within the VENTURES Project (2011-8/1) and TEAM Project (2012-9/4), co-financed by the European Union, Regional Development Fund, is highly acknowledged by TB and SW, respectively. Some equipment were purchased with the financial support of the European Regional Development Fund in the framework of the Polish Innovation Economy Operational Program (contract no. POIG.02.01.00-12-023/08).

References

- 1 M. Aresta and G. Forti, Eds., *Carbon Dioxide as a Source of Carbon*, Springer Netherlands, Dordrecht, 1987.
- 2 M. M. Maroto-Valer, Ed., in *Developments and Innovation in Carbon Dioxide (CO₂) Capture and Storage Technology*, Woodhead Publishing, 2010, vol. 1, pp. i–iii.
- 3 E. Barton Cole and A. B. Bocarsly, in *Carbon Dioxide as Chemical Feedstock*, ed. M. Aresta, Wiley-VCH Verlag GmbH & Co. KGaA, 2010, pp. 291–316.
- 4 M. Aresta, A. Dibenedetto and E. Quaranta, *Reaction Mechanisms in Carbon Dioxide Conversion*, Springer-Verlag Berlin Heidelberg, 2015.
- 5 Pat. Appl. MI2013A001135, 2013.

- 6 A. Dibenedetto, P. Stufano, W. Macyk, T. Baran, C. Fragale, M. Costa and M. Aresta, *ChemSusChem*, 2012, **5**, 373–378.
- 7 M. Aresta, A. Dibenedetto, T. Baran, A. Angelini, P. Łabuz and W. Macyk, *Beilstein J. Org. Chem.*, 2014, **10**, 2556–2565.
- 8 D. W. Bahnemann, J. Moenig and R. Chapman, *J. Phys. Chem.*, 1987, **91**, 3782–3788.
- 9 J. Lee and W. Choi, *J. Phys. Chem. B*, 2005, **109**, 7399–7406.
- 10 A. A. Ismail and D. W. Bahnemann, *Green Chem.*, 2011, **13**, 428–435.
- 11 A. A. Ismail and D. W. Bahnemann, *J. Phys. Chem. C*, 2011, **115**, 5784–5791.
- 12 T. Baran, A. Dibenedetto, M. Aresta, K. Kruczała and W. Macyk, *ChemPlusChem*, 2014, **79**, 708–715.
- 13 T. Baran, S. Wojtyła, A. Dibenedetto, M. Aresta and W. Macyk, *Appl. Catal. B Environ.* DOI:10.1016/j.apcatb.2014.09.052
- 14 T. Baran, S. Wojtyła, A. Dibenedetto, M. Aresta and W. Macyk, 2015 data not published
- 15 L. G. Warde, *Organic Chemistry*, Hardcover, 2009.
- 16 R. Morrison and R. Boyd, *Organic chemistry*, Hardcover, 1992.
- 17 S. J. Blanksby and G. B. Ellison, *Acc. Chem. Res.*, 2003, **36**, 255–263.
- 18 K. M. Ervin, S. Gronert, S. E. Barlow, M. K. Gilles, A. G. Harrison, V. M. Bierbaum, C. H. DePuy, W. C. Lineberger and G. B. Ellison, *J. Am. Chem. Soc.*, 1990, **112**, 5750–5759.
- 19 G. da Silva, C.-H. Kim and J. W. Bozzelli, *J. Phys. Chem. A*, 2006, **110**, 7925–7934.
- 20 H. Kisch, *Semiconductor Photocatalysis: Principles and Applications*, Wiley-VCH, 2015.
- 21 F. Osada, H. Furukawa, M. Matsubara, T. Imai and K. Tsukiyama, Fukuoka, 2012.
- 22 R. Künneth, C. Feldmer, F. Knoch and H. Kisch, *Chem. – Eur. J.*, 1995, **1**, 441–448.
- 23 H. Keck, W. Schindler, F. Knoch and H. Kisch, *Chem. – Eur. J.*, 1997, **3**, 1638–1645.
- 24 A. Reinheimer, A. Fernández and H. Kisch, *Z. Für Phys. Chem.*, 1999, **213**, 129–133.
- 25 G. Hörner, P. Johne, R. Künneth, G. Twardzik, H. Roth, T. Clark and H. Kisch, *Chem. – Eur. J.*, 1999, **5**, 208–217.
- 26 T. Baran, A. Dibenedetto, M. Aresta, K. Kruczała and W. Macyk, *ChemPlusChem*, 2014, **79**, 708–715.